

RESEARCH OF DEPOSIT ACCUMULATED ON HEAT EXCHANGE SURFACES IN THE LIGHT OF THERMAL DEGRADATION OF HEAT EXCHANGE APARATUS OF STEAM POWER PLANTS

PART I: STUDY OF REAL SEDIMENTS

Tomasz Hajduk
Gdynia Maritime University, Poland

ABSTRACT

The presence of deposits on heat exchange surfaces in condensers and regenerative exchangers of ship and land steam power plants is always connected with the increase of the wall temperature on the water vapor side due to additional thermal resistances resulting from accumulated deposits. This increase always results in an increase in the condensing pressure, which results in the deterioration of the condensation process of the water vapor, leading to thermal degradation of a given heat exchanger. In addition, the resulting deposits form unevenness with a diversified, often stochastic, geometric structure of the surface layer surface, whose measure is most often the roughness parameters, describing the geometric structure of the surface. In addition, the increase in surface roughness of the heat transfer surface on the water vapor side promotes the formation of a thicker layer of condensate, thus worsening the organization of condensate runoff, which results in interference of the thermal degradation phenomenon of a given heat exchange apparatus. As a result, these phenomena lead to a reduction in the efficiency of a given thermal system, and thus entail an increase in the costs of energy conversion and consequently cause an increased degradation of the natural environment. In the article, based on the results of the author's own experimental research, the types of pollution accumulating on heat exchange surfaces on the water vapor side of heat exchange apparatus in marine and land steam power plants and quantitative measures of the unevenness of the surface layer of these sediments are presented.

Keywords: steam power plants, heat exchangers, deposits, spectral analysis, surface geometric texture

INTRODUCTION

In the theory of heat exchange, the term “fouling” according to Knudsen, is designated as a substance that accumulates on the surface of heat exchange, which at the same time puts additional thermal resistance in the heat transfer processes. As a result, thermal degradation of a given exchanger occurs [12]. Pollutants are often referred to as deposits, although the name, as Taborek notes [21], should belong only to impurities occurring in the form of a solid.

In spite of maintaining the recommended methods of chemical correction of feed water, boiler water, condensate and water vapor, during the operation of power units of steam power plants, sedimentary phenomena occur and

corrosion processes in water-steam cycles [22]. As a result of these processes, deposits are deposited on the heat exchange surfaces both on the water side and on the steam side. The serious operational difficulties resulting from this influence the setting of increasingly stringent requirements in relation to the quality of water and the quality of water vapor [2]. Moreover, filling the cycle with water properly cleaned and chemically prepared does not guarantee proper operation of steam power plant devices, because high temperature and pressure, as well as high thermal load of the heat exchange surface cause a series of complex physicochemical changes, changing water properties and its reactivity to construction materials of energy devices. The mechanism of these changes is not completely recognized. Therefore, it is necessary to

constantly check the quality of the circulating medium and correct its composition so that the devices can be operated in accordance with the guidelines of designers and manufacturers. Typically, the processes of deposit formation on heat exchange surfaces and corrosion processes are closely related [20].

The chemical composition of deposits formed on the water side depends also to a large extent on the construction type of the heat exchanger itself and its function (condensers, low and high pressure regeneration heat exchangers) [21]. The basic contaminants present in water include salts and gases dissolved in it, as well as some organic substances, i.e. calcium, sodium, potassium, magnesium, manganese, iron salts, calcium sulfates, calcium chloride, silica and silicates (so-called water glass). In addition, impurities may occur in the liquid phase (turbine oil) and gas, as so-called non-condensing gases (air) [19].

In the literature on the subject concerning deposits from the steam heat exchange surface of low and high pressure regeneration heat exchangers as well as condensers of land and sea steam power plants, it is shown that these types of sediments mainly consist of iron oxides in the form of: Fe_3O_4 , $FeO \cdot Fe_2O_3$, Fe_2O_3 and FeO and copper compounds. The percentage of these compounds in the deposits varies and depends on the material of the heat exchanger pipe [15].

An additional problem in the operation of heat exchangers used in energy block systems are microorganisms that form biological pollutants in the form of deposits (biofouling), e.g. mussels, crustaceans, fungi, algae and bacterial colonies. The important microorganisms responsible for corrosion phenomena include bacteria oxidizing iron and manganese compounds: *Thiobacillus ferrooxidans*, *Ferrobacillus ferrooxidans*, *Metalogenium symbioticum* [9].

In addition, the resulting pollutants usually form unevenness with different geometric structure of the surface layer surface both on the heat transfer surfaces of shell and tube exchangers as well as plate exchangers [11, 14, 23]. An interesting fact is that the irregularity of the external heat exchange surface created by the depositing deposits, on the one hand, may intensify the heat exchange process, and on the other hand may contribute to an additional increase in thermal degradation of the exchanger [6, 8, 24]. For example, Brahim et al [3] studied the influence of the shape of the geometric structure of the deposit surface collected from the cooling water side of the heat exchanger on the course of time characteristics of thermal resistance of impurities. These tests have shown that a greater unevenness of heat exchange surfaces from the cooling water side of the exchanger causes a smaller increase in the thermal resistance of pollutants over time, however, the increase in roughness is also combined with an increase in flow resistance.

On the other hand, the studies of Förster and Bohnet [8] regarding the influence of surface heat exchange surface roughness on the course of time characteristics of thermal resistance showed that larger irregularities of this surface cause a significant increase in thermal resistance of pollutants over time. For example, in the initial stage of salt precipitation

from water, in the so-called induction time τ_{ind} , they are deposited in the form of flakes tightly adhering to the surface of the pipe. They are a form of microchips, which on one hand develop the surface of heat exchange, and on the other, act as flow turbulizers breaking the laminar boundary layer, which results in the intensification of heat exchange. Therefore, some authors call τ_{ind} time as the period of intensification of heat exchange [26]. It is worth adding that extension of the τ_{ind} period is one of modern strategies against thermal degradation of heat exchangers [8].

The influence of wall impurities on a single pipe is often taken into account by means of corrections, referred directly to the calculated coefficient of heat transfer α_v from the condensing side of steam. Especially when it is difficult to distinguish the influence of the thermal resistance of the deposit layer from the influence of surface roughness. For example, Kutateladze recommends correction of the coefficient α_v with the indicator ϵ (tab.1), the value of which depends on the type of material and the condition of the pipe surface. However, it is a relationship presented only in a descriptive way. For example, for a steel pipe, covered with a thin deposit of deposit, the index ϵ is 0.67 - however, the author does not specify how thick the deposit layer is and what is the irregularity of its surface [10].

Tab. 1. The values of the correction factor ϵ depending on the material and condition of the pipe surface for the heat transfer coefficient on the water vapor side, according to [10]

| ϵ | Pipe type |
|------------|---|
| 1.36 | surface ground to a mirror shine |
| 1.00 | smooth brass pipes |
| 0.83 | Normal or drawn steel pipes |
| 0.79 | pipes coarsely cleaned with sandpaper |
| 0.67 | steel pipes covered with thin deposit coating |

In addition, the increase in surface roughness of the heat transfer surface on the water vapor side promotes the formation of a thicker layer of condensate, thus worsening the so-called conditions of run-off during the condensation process of water vapor. This phenomenon can be explained by the fact that the formed deposits on the side of the pair create, in a sense, quasi-ribs, which can lead to a process of flooding intercostal canals well-known in literature. This phenomenon has an adverse effect on the operation of a single pipe, because the bottom layer of condensation, with a thickness approximately equal to the height of the ribs, constitutes an additional thermal resistance [4, 25].

Summing up, the issues aimed at identifying substances constituting deposits on heat exchange surfaces of heat exchangers of steam power plants and the quantitative description of the structure of the surface layer of deposits are a vital research issue. Knowledge of physico-chemical properties and the structure of the surface layer of the resulting deposits supports the quality of mathematical models, taking into account the features of thermal degradation, resulting from the deposition of pollutants on heat exchange surfaces of heat exchangers of steam power plants. It is worth emphasizing that these models have extremely important

practical importance, as they are used in thermal and flow diagnostics and in the planning of repair actions of these devices [5, 13, 27].

The author of this work carried out experimental research on deposits formed on the surfaces of heat exchange on the water vapor side. These studies were carried out in two stages, the first of which concerned the identification of chemical compounds of deposits, the second – the assessment of the surface layer of deposits.

RESEARCH ON THE CHEMICAL COMPOSITION OF DEPOSITS

In the research identifying the chemical composition of deposits accumulating on the heat exchange surfaces in steam power plants, the spectral analysis method based on the analysis of the X-ray spectrum was used. The purpose of this analysis is to detect elements or chemical compounds of the test sample (qualitative analysis) and to determine the quantitative composition of the sample by measuring the intensity of radiation at a specific wavelength (quantitative analysis) [7].

RESEARCH METHODOLOGY

Spectral analysis of the chemical composition of deposits was carried out by measuring the emission of characteristic EDS radiation, with the use of the semi-quantitative method [7]. The tests were carried out at the Department of Materials Engineering at the Faculty of Mechanical Engineering at the Gdańsk University of Technology. To identify the elemental composition of the tested samples and determine their quantitative composition, high-quality scientific-research equipment was used, i.e. an environmental scanning microscope type FEI XL 30 ESEM manufactured by Philips. The basic data of this device is included in table 2 [29].

Experimental tests were carried out for individual pipes from heat exchangers of three different steam power plants, which were coded as: RFS#02, RFS#07, RFS#12. Basic information about research materials along with their sensory characteristics is given in Table 3.

Tab. 2. Nominal characteristics of the scanning microscope, Philips, type FEI XL 30 ESEM, acc. [29]

| Feature | Characteristic |
|-------------------|---|
| Accuracy | < 1% measured quantity |
| Operating mode | I. High vacuum – conductive specimen; II. Low vacuum – non-conductive specimen |
| Control | Computer, Windows® NT environment software |
| Electronic cannon | Tungsten cathode with automatic setting, saturation and alignment |
| Resolution | 3.5 nm @ 30 kV (low and high vacume); 15 nm @ 3 kV (low vacume) |
| Detectors | Built-in EDX spectrometer detector |
| Magnification | 6×1 200 000 high vacume; 250×400 000 environmental mode |
| Vacuum system | Turbomolecular pumps, vacuum recovery time: a) high: 3.5 min, b) low: 2.5 min. |

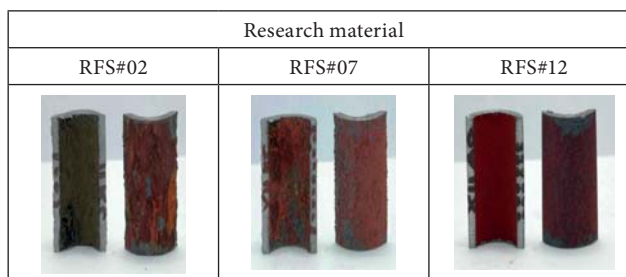
| Feature | Characteristic |
|---|---|
| Presentation and recording of the image | 15 „LCD monitors, 7” HD photomonitor with a 35mm SLR camera, digital image recording: HDD, FDD, CDR |

Tab. 3. Sensory characteristics of sediments formed on the water vapor side of the tested samples RFS#02, RFS#07, RFS#12, according to [self.]

| Sample | Color | Roughness | Origin |
|--------|--------------|----------------|----------------------------------|
| RFS#02 | brown-yellow | irregular | HR-HP; EC 100 MW; Donator: KR |
| RFS#07 | rusty-blue | fairly regular | HR-LP; E 200 MW; Donator: KR |
| RFS#12 | purple | regular | HR-LP; E 100 MW; Donator: AG |

Samples for testing were prepared in accordance with the applicable experimental measurements procedure in quantitative X-ray microanalysis. The limitations resulting from the geometry of the environmental chamber of the Philips FEI XL 30 ESEM scanning microscope were taken into account. Table 4 shows photos of RFS#02, RFS#07 and RFS#12 deposit samples. They were made from a tripod with a Nikon D70S camera with a MicroNikkor 105 mm – 1:2.8D lens (settings: white balance – user, ISO – 200, diaphragm – 32, time – 1s).

Tab. 4. Photographs of deposit samples for testing the chemical composition by spectral analysis, according to [self.]



RESULTS OF SPECTRAL ANALYSIS

The results of research on spectral analysis of the sediments of the tested samples RFS#02, RFS#07 and RFS#12 are presented in Table 5.

Tab. 5. Results of spectral analysis for deposit samples from steam engine heat exchangers, according to [self.]

| RFS#02 | | RFS#07 | | RFS#12 | |
|---------|--------|---------|--------|---------|--------|
| Element | Wt % | Element | Wt % | Element | Wt % |
| O K | 21.92 | O K | 20.21 | O K | 18.57 |
| Si K | 0.34 | Si K | 0.72 | Fe K | 79.30 |
| P K | 0.53 | Mn K | 0.62 | Co K | 2.12 |
| S K | 0.38 | Fe K | 64.84 | Total | 100.00 |
| Mn K | 1.38 | Cu K | 13.61 | | |
| Fe K | 75.45 | Total | 100.00 | | |
| Total | 100.00 | | | | |

An exemplary spectrogram of the tested sediments for the RFS#07 sample is shown in Figure 1.

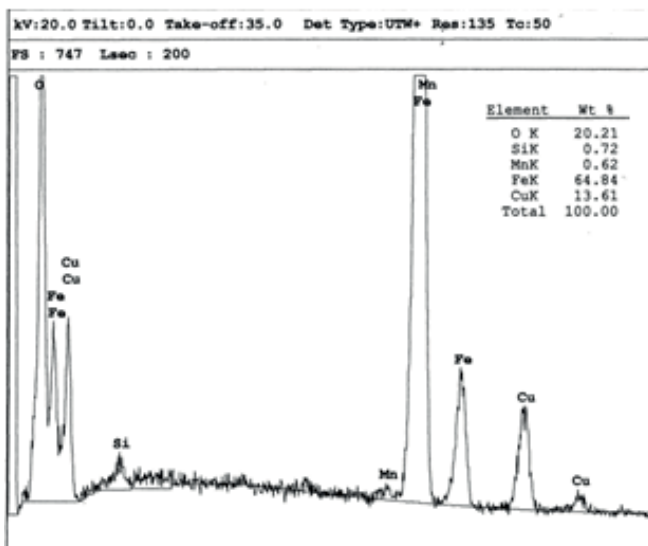


Fig. 1. Spectrograph of the sample deposits of RFS#07 obtained with the Philips EI XL 30 ESEM scanning microscope, according to [self]

INTERPRETATION OF TEST RESULTS

The identification of deposits of the analyzed samples was based on the stoichiometric analysis method [17]. Comparisons of the number of moles of the forecasted compounds with the theoretical values of quantitative relations that exist in chemical compounds have been made, i.e. in compounds that, according to literature, potentially constitute deposits on the water vapor side of heat exchange surfaces of heat exchange devices in land and marine steam power plants. The theoretical values of stoichiometric relations sr_T in chemical compounds forming deposits on heat exchange surfaces of heat exchangers in steam power plants are presented in Table 6 [17].

Tab. 6. Values of stoichiometric relations sr_T (theoretical) chemical compounds, according to [17]

| Deposit | FeO | Fe ₂ O ₃ | CuO | Cu ₂ O |
|-----------------|----------|--------------------------------|----------|-------------------|
| relation sr_T | Fe:O 1:1 | Fe:O 2:3 | Cu:O 1:1 | Cu:O 2:1 |
| value sr_T | 1.00 | 0.67 | 1.00 | 2.00 |

The number of real $n_{S_{Ei}}$ moles of the i -th element E contained in the sample was determined based on the dependence:

$$n_{S_{Ei}} = \frac{m_{Ei}}{M_{Ei}} \quad (1)$$

where:

m – mass of the E_i element in the sample [g],
 M – the molar mass of the E_i element [g/mol].

The molar ratio $mrs_{Ei:Ej}$ between i -th and j -th element in the sample is expressed:

$$mrs_{Ei:Ej} = \frac{n_{S_{Ei}}}{n_{S_{Ej}}} \quad (2)$$

An exemplary analysis of the identification of chemical compounds constituting deposits was carried out for the RFS#07 sample. Taking into account the results of tests from tab. 5 and formula 1, the number of moles n_{S_p} of the elements is:

$$n_{S_O} = \frac{m_O}{M_O} = \frac{20.21}{16.00} = 1.263;$$

$$n_{S_{Fe}} = 1.161; n_{S_{Cu}} = 0.214;$$

$$n_{S_{Si}} = 0.026; n_{S_{Mn}} = 0.011.$$

On the basis of formula 2 and the values of moles determined above, and taking into account theoretical values from table 6 of stoichiometric ratios, the following chemical compounds were evaluated as the tested deposit:

– iron compounds,

$$mrs_{Fe:O} = \frac{n_{S_{Fe}}}{n_{S_O}} = \frac{1.161}{1.263} = 1.00$$

It was identified as iron oxide (II). For further analysis, 0.102 moles of oxygen remain at the disposal ($0.102 = 1.263 - 1.161$). Hence, another compound was sought among copper oxides:

– copper compounds,

$$mrs_{Cu:O} = \frac{n_{S_{Cu}}}{n_{S_O}} = \frac{0.214}{0.102} = 2.09 \approx 2.00$$

It was estimated that it is copper oxide (I). The remaining elements (Si, Mn) occurred in trace amounts and could be “broken” from the tube material during the test. All results of the identification of chemical compounds included in the deposits on heat exchange surfaces of the tested samples are included in Table 7.

Tab. 7. Identification of chemical compounds constituting deposits of the tested samples RFS#02, RFS#07, RFS#12, according to [self]

| Sample | Number of moles | Recognition |
|--------|--|---------------------------|
| RFS#02 | $n_{S_O}=1.37, n_{S_{Fe}}=1.35,$ other elements in trace amounts | FeO |
| RFS#07 | $n_{S_O}=1.26, n_{S_{Fe}}=1.16, n_{S_{Cu}}=0.21,$ other elements in trace amounts | FeO, Cu ₂ O |
| RFS#12 | $n_{S_O}=1.16, n_{S_{Fe}}=1.42,$ other elements in trace amounts | not determined |

EXAMINATION OF THE SURFACE LAYER OF DEPOSITS

The actual surface of the solid body is the boundary between it and the surrounding center. It is an integral, external part of the surface layer. The top layer, which was created under certain technological conditions, is called technological surface layer. However, the layer that was created under operating conditions is the so-called operational top layer [18]. The structure of the external surface is determined by the geometric structure of the surface (SGP). It is assumed that the state of SGP consists of four classes of irregularities, I) shape outlines, II) surface waviness, III) surface roughness,

and IV) surface microroughness [1, 16]. In the experimental studies, the author assumed to determine as equivalent: the surface layer of deposits and the heat exchange surface on the water vapor side of the steam engine heat exchangers.

RESEARCH METHODOLOGY

The measure of irregularities in the surface layer of deposits can be characterized by a set of parameters whose values depend on the properties of the material constituting the deposit and on the conditions in which the deposit was formed. The assessment of the geometric structure of the deposit surface was made on the basis of the theory that is valid for the assessment of surface microgeometry for machinery elements that cooperate with each other. The issues related to metrology, shaping and the influence of the geometric structure of the surface on the operational properties of machines are a very complex problem and considerably extend beyond the scope of research undertaken by the author of this article [1, 16, 18]. In own research, the author limited himself to the use of several basic parameters in the field of the assessment of the geometric structure of the surface for the unevenness of the 3rd class of the surface layer. The following roughness measures [1, 28] were accepted for the description of the tests:

1. The average arithmetic deviation of the profile Ra :

$$Ra = \frac{1}{N} \sum_{i=1}^N |Y_i| \quad (3)$$

2. The average square deviation of the profile Rq :

$$Rq = \sqrt{\frac{1}{N} \sum_{i=1}^N Y_i^2} \quad (4)$$

3. The maximum height of the profile Rz :

$$Rz = \frac{1}{n} \sum_{i=1}^n Rz_i \quad (5)$$

4. The maximum height of the peak Rp :

$$Rp = \frac{1}{n} \sum_{i=1}^n Rp_i \quad (6)$$

5. Maximum height of the recess Rv :

$$Rv = \frac{1}{n} \sum_{i=1}^n Rv_i \quad (7)$$

6. The average width of the profile elements Rsm :

$$Rsm = \frac{1}{m} \sum_{i=1}^m Xs_i \quad (8)$$

where:

- Y_i – absolute values of profile's deviations R ,
- Rz_i – the largest height of the roughness profile for the elementary section,
- Rp_i – the largest elevation of the roughness profile for the elementary section,
- Rv_i – the largest depression of the roughness profile for the elementary section,
- Rsm – the average value of the width of the Xs profile elements inside the elementary segment,
- n – number of elementary sections.

The texture parameter K of the top deposit layer was calculated by the Förster and Bohnet formula:

$$K = (Rz \cdot Rsm)^{-1} \quad (9)$$

Förster and Bohnet [8] showed in their research that the texture parameter K has a significant effect on the value of the induction time τ_{ind} . They obtained an empirical positive correlation between the time of deposit excitation τ_{ind} (in hours) and the texture parameter K assuming values from 0 to $0.8E10 \text{ m}^{-2}$:

$$\tau_{ind} = 7.0789 \cdot 10^{-9} \cdot K + 12.8 \quad (10)$$

The shortest period τ_{ind} was characterized by the surface with the highest irregularity of the structure of the surface layer (small K values), while the longest period τ_{ind} was characterized by the surface with the least irregularity (high K values).

RESEARCH STAND

Roughness measurements were made by contact method, two-dimensional surface registration technique in the Laboratory of Cavitation of the Center of Liquid Mechanics at IMP PAN in Gdańsk. The test stand for surface unevenness consisted of two main parts: a roughness measuring instrument - a surface-contact profilometer of the Mitutoyo manufacturer, type SJ-301 (fig. 2) and Mitutoyo ver. 3.20 for acquisition and processing of measurement data [30].

Each measurement of the surface roughness of the deposit was preceded by a visual assessment of the test sample, thanks to which the direction of the measurement was determined and the measurement section was selected. Measurements of microgeometry of the surface of the samples were carried out on their cylindrical surface, in the longitudinal direction to the axis of the samples. For each sample, measurements were taken for three different measurement sections.



Fig. 2. Mitutoyo SJ-301 Surface Roughness Tester stand, by [self]

These sections were selected from two cross-sections of the research material. They arose from the intersection of the surface of the cylindrical tube with the plane at the central angles: $\alpha=0^\circ$, $\beta=120^\circ$ and $\gamma=240^\circ$ (Figure 3). The value of the arithmetic mean of the parameters measured in the given planes was used for the analysis.

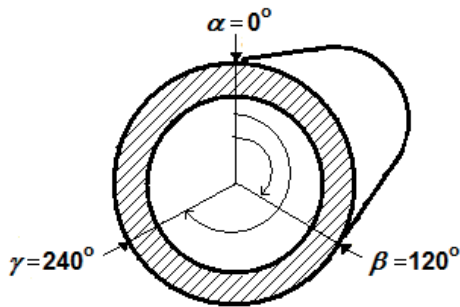


Fig. 3. Plots defining the places of roughness measurement of the tested deposit, according to [self]

To describe the microgeometry of the surface layer of deposits, the following settings were selected in the Mitutoyo ver. 3.20: measured profile R , amplitude permeation filter GAUSS, length of the elementary measuring section $l_r=0.8$ mm, total measuring length $l_n=4.0$ mm (times $n=5$), length of the run-up section $\lambda_c/2=0.4$ mm and length of the coasting section $\lambda_c/2=0.4$ mm, while λ_c is the filter cut-off length equal to l_r [30].

Tab. 8. Measured in the planes of the center angles α , β , γ and averaged (av) values of the surface profile parameters of the tested samples RTS#00, RFS#02, RFS#07 and RFS#12, "b.d." no data, according to [self]

| Measure [μm] | Research material | | | | | | | | | | | | | | | |
|------------------------------|-------------------|----------|---------|----------|--------|----------|---------|----------|--------|----------|---------|----------|--------|----------|---------|----------|
| | RTS#00 | | | | RFS#02 | | | | RFS#07 | | | | RFS#12 | | | |
| | av | α | β | γ | av | α | β | γ | av | α | β | γ | av | α | β | γ |
| R_a | 0.96 | 0.53 | 1.14 | 1.21 | 7.76 | 9.61 | 7.11 | 6.57 | 7.07 | 4.45 | 11.78 | 4.98 | 6.22 | 4.24 | 8.57 | 5.84 |
| R_q | 1.33 | 0.73 | 1.59 | 1.69 | 9.95 | 12.65 | 9.38 | 7.81 | 8.85 | 5.60 | 14.17 | 6.79 | 7.78 | 5.27 | 10.55 | 7.52 |
| R_z | 6.62 | 4.47 | 7.52 | 7.88 | 40.78 | 54.10 | 38.27 | 29.96 | 37.17 | 23.10 | 54.95 | 33.47 | 34.81 | 23.31 | 49.02 | 32.09 |
| R_p | 3.11 | 1.99 | 3.79 | 3.54 | 19.83 | 23.02 | 20.84 | 15.65 | 17.23 | 11.61 | 25.43 | 14.64 | 17.68 | 12.63 | 24.08 | 16.34 |
| R_v | 3.52 | 2.47 | 3.73 | 4.35 | 20.94 | 31.08 | 17.43 | 14.31 | 19.94 | 11.49 | 29.51 | 18.83 | 17.12 | 10.68 | 24.94 | 15.75 |
| R_{sm} | 161 | 161 | b.d. | b.d. | b.d. | b.d. | b.d. | b.d. | 330 | 279 | 382 | b.d. | 255 | 200 | 368 | 198 |

The deposit roughness tests were carried out on specially prepared samples, due to constraints conditioned by the maximum permissible length of the profilograph measuring section ($l_{n,max} \leq 12.5$ cm). In addition, an important problem was the leveling of the tested material, when its length is much higher than $l_{n,max}$. The tests were carried out for samples, of which one RTS#00 was free from deposits (reference sample), while the remaining three samples: RFS#02, RFS#07 and RFS#12 came from the heat exchange apparatus for regeneration of low and high pressure steam power plants.

RESULTS OF THE SURFACE LAYER TESTING

After reaching the stability status within each measurement series, an electronic test protocol was prepared by a measurement data acquisition system. Table 8 shows the measured roughness parameters and their average values. Moreover, scanning photos of the surface layer of the tested samples were recorded using the Philips FEI XL 30 ESEM scanning microscope (Fig. 4, Fig. 5, Fig. 6). The measure of irregularities of the surface layer of heat exchange surface on the water vapor side for a pipe without sediments (sample RTS#00) and for pipes with sediments (samples RFS#02, RFS#07, RFS#12) was determined based on the texture parameter K and presented in Table 9. In addition, taking into account the correlation (10), the hypothetical deposit excitation time τ_{ind} for a pipe without deposit (reference, RTS#00) was estimated at about 20 hours.

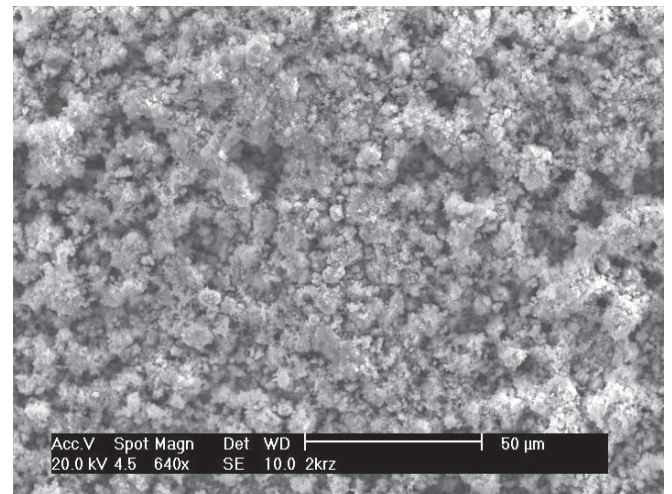


Fig. 4. Scanning image of the surface layer of the sample deposits of the RFS#02 in an enlargement of 640x, according to [self]

Tab. 9. Values of the texture parameter K of the top layer of the deposits of the tested samples RTS#00, RFS#02, RFS#07 and RFS#12, according to [self]

| Texture parameter | Research material | | | |
|------------------------------|-------------------|--------|--------|--------|
| | RTS#00 | RFS#02 | RFS#07 | RFS#12 |
| $K \times 10^{-10} [m^{-2}]$ | 0.094 | b.d. | 0.008 | 0.013 |

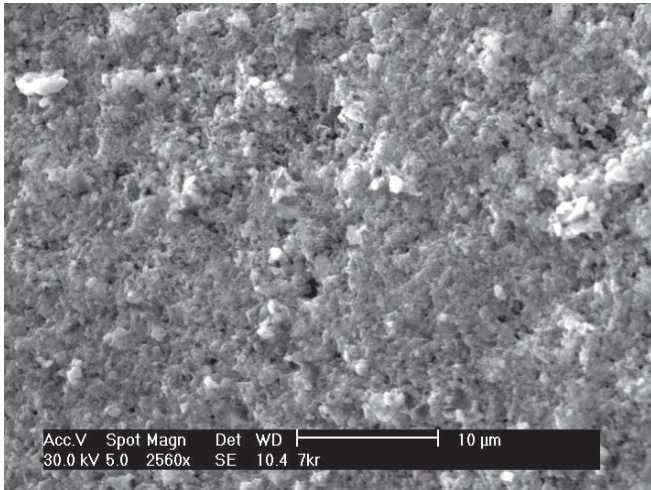


Fig. 5. Scanning photo of the surface layer of the sample deposits of RFS#07 at 2560x enlargement, according to [self]

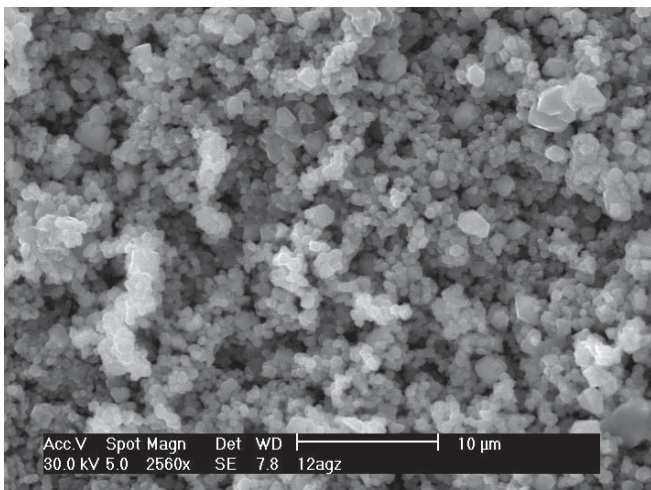


Fig. 6. Scanning photo of the surface layer of the sample deposits of RFS#12 at 2560x enlargement, according to [self]

DISCUSSION

Tests identifying the chemical composition of sediments accumulating on the water vapor side on heat exchange surfaces of heat exchangers of steam power plants have shown that the elements with the largest mass fraction were: iron, oxygen and copper. The results of the spectral analysis also showed the presence of trace elements of, i.e. cobalt, manganese, silicon, phosphorus and sulfur. The reason for the presence of these elements on spectrograms could be their removal from the tube material. On the basis of the obtained

spectra of the chemical composition of the deposits studied, an attempt was made to identify the chemical compounds that create them. Two compounds have been identified, i.e. iron oxide (II) (more frequently occurring) and copper oxide (I). It should be added that the shape of the spectral analysis results was influenced by the type of method adopted – a semi-quantitative method without a pattern. This method is considered to be less accurate than the full quantitative method with the pattern, nevertheless, the obtained results of empirical studies confirmed compliance with the results presented in literature on deposits accumulating on the water vapor side on heat exchange surfaces of land heat and marine steam power plants.

The second stage of the empirical research concerned the assessment of the structure of the surface layer of the tested deposits. The tests showed that the pipe without deposits was characterized by the lowest vertical irregularity of the surface, i.e. the Ra and Rz values for the RTS#00 sample reached values by an order of magnitude smaller than those for pipes with deposits. The results of the research also confirmed greater variation in the structure of the surface layer for pipes covered with deposits, i.e. RFS#07 and RFS#12. The texture parameter K of the pipes with deposits was smaller than the parameter K for the pipe without deposits, respectively about 12 and 7 times (in the case of the RFS#02 sample, the Rsm parameter and therefore the parameter K) could not be determined. Moreover, comparing the texture parameter K between the deposits of the RFS#07 and RFS#12 pipes, it was found that the irregular structure of the top layer, about 60% irregular, was characterized by the RFS#12 pipe. In operational practice, this state of things may result in a significant deterioration of the organization of condensate runoff from a single pipe. This phenomenon occurs due to flooding of intercostal microspheres, while generating additional thermal resistance. This resistance ultimately leads to an increase in the thermal degradation of a given heat exchange apparatus.

CONCLUSIONS

In conclusion, the influence of the presence of deposits accumulated on heat exchanger surfaces of steam-exchangers on the condensation of water vapor, due to the overlap of many phenomena at the same time, is a large issue in terms of research and complexity in the phenomenological explanation. In the author's conviction, a more detailed recognition of the type of accumulating deposits on heat exchange surfaces contributes to a more precise determination of their physical and chemical properties (quantitative aspect). On the other hand, systematic studies of the structure of the surface layer of deposits based on roughness parameters (quantitative aspect) can significantly contribute to the enhancement of the description of the phenomenon of steam condensation of energy heat exchange apparatus. The above results in the potential improvement of mathematical models of heat exchange devices, which ultimately leads to improvement of procedures for handling heat exchangers

of steam power plants according to the technical condition with control of parameters.

LITERATURE

1. Adamczak S.: Ocena chropowatości i falistości powierzchni. Informacje podstawowe. *Mechanik*, 2005, nr 5-6, s. 492-495.
2. Bednarek G., Maciejko M.: Reżim chemiczny stosowany w eksploatacji bloków energetycznych o mocy 360 MW w Elektrowni Bełchatów. *Energetyka*, 2003, rok XLVIII, nr 5, str. 309-321.
3. Brahim F., Augustin W., Bohnet M.: Numerical simulation of the fouling structured heat transfer surfaces. ECI Conference on Heat Exchanger Fouling and Cleaning. *Fundamentals and Applications*, 2003, pp. 121-129.
4. Butrymowicz D.: Influence of fouling and inert gases on the performance of regenerative feedwater heaters. *Archives of Thermodynamics*, 2001, Vol. 23, No. 1-2, pp. 127-140.
5. Butrymowicz D., Głuch J., Hajduk T., Trela M., Gardzilewicz A.: Analysis of fouling thermal resistance of feed-water heaters in steam power plants. *Polish Maritime Research*, 2009, Special issue S1, pp. 3-8.
6. Butrymowicz D., Hajduk T.: Zagadnienia degradacji termicznej wymienników ciepła. *Technika chłodnicza i klimatyzacyjna*, 2006, rok XIII, nr 3(121), s. 111-117.
7. Cygański A.: Metody spektroskopowe w chemii analitycznej. WNT, 1993, Warszawa.
8. Förster M., Bohnet M.: Modification of the interface crystal/heat transfer surface to reduce heat exchanger fouling. (ed.) Müller-Steinhagen H., *Heat Exchanger Fouling. Fundamental Approaches & Technical Solutions*, 2002, pp. 27-34.
9. Giebień R.: Biokorozja w energetyce. *Energetyka*, 2002, nr 8, str. 579-586.
10. Hobler, T.: Ruch ciepła i wymienniki. WNT, 1986, Warszawa.
11. Kazi S.N., Duffy G.G., Chen X.D.: A study of fouling and fouling mitigation on smooth and roughened metal surfaces and a polymeric material. (ed.) Müller-Steinhagen H., *Heat Exchanger Fouling. Fundamental Approaches & Technical Solutions*, 2002, pp. 65-72.
12. Knudsen J.G.: Fouling in Heat Exchangers. Overview and Summary. (ed.) Hewitt G.F., *Handbook of heat exchanger design*, Begell House Inc., 1992, New York, pp. 3.17.1.1-7.5.
13. Krzyżanowski J.A., Głuch J.: Diagnostyka cieplno-przepływowa obiektów energetycznych. Wydawnictwo IMP PAN, 2004, Gdańsk.
14. Kukulka D.J., Devgun M.: Fouling surface finish evaluation. *Applied Thermal Engineering*, 2007, Vol. 27, pp. 1165-1172.
15. Łodej M.: Nowa metoda chemicznego oczyszczania regeneracyjnych podgrzewaczy wysokoprężnych po stronie parowej. *Energetyka*, 2002, rok XLVII, nr 10/11, str. 809-811.
16. Nowicki, B.: Chropowatość i falistość powierzchni. WNT, 1991, Warszawa.
17. Pauling L., Pauling P.: *Chemia*. Wydawnictwo Naukowe PWN, 1998, Warszawa.
18. Senatorski J. K.: Podnoszenie tribologicznych właściwości materiałów przez obróbkę cieplną i powierzchniową. Instytut Mechaniki Precyzyjnej, 2003, Warszawa.
19. Stańda J.: Woda do kotłów parowych i obiegów chłodzących siłowni cieplnych. WNT, 1999, Warszawa.
20. Śliwa A.: Wpływ stopnia czystości pary na procesy korozyjne występujące w części przepływowej turbiny. *Energetyka*, 2003, nr 6, str. 407-410.
21. Taborek J.: Effects of Fouling and Related Comments on Marine Condenser Design. Marto P.J., Nunn R.H. (eds.): *Power Condenser Heat Transfer Technology*. Hemisphere Publishing Co., 1981, pp. 425-430.
22. Twardowski S., Maciejko M., Kozupa M.: Nowoczesne środki aminowe do korekcji czynnika roboczego w obiegach bloków energetycznych. *Energetyka*, 2000, Vol. LIV, nr 9, str. 75-79.
23. Wajs J., Milkielewicz D.: Influence of metallic porous microlayer on pressure drop and heat transfer of stainless steel plate heat exchanger. *Applied Thermal Engineering*, 2016, Vol. 93, pp. 1337-1346.
24. Wajs J., Milkielewicz D.: Effect of surface roughness on thermal-hydraulic characteristics of plate heat exchangers. *Key Engineering Materials*, 2014, Vol. 597, pp. 63-74, doi: 10.4028/www.scientific.net/KEM.597.63
25. Webb R.L.: The use of enhanced surface geometries in condensers. An overview. (eds) Marto P.J., Nunn R.H.: *Power Condenser Heat Transfer Technology*, 1981, pp. 353-366.
26. Xu Z.M., Wang J.G., Chen F.: A new predictive model for particulate fouling. (ed.) Bott T.: *Understanding Heat*

Exchanger Fouling and Its Mitigation. 1999, New York, pp. 185-192.

27. Zbroińska-Szczuchura E., Dobosiewicz J.: Uszkodzenia i diagnostyka wymienników ciepła w elektrociepłowniach. Energetyka, 2004, nr 12, str. 796-800.

28. DIN-EN ISO 4288, GPS – Surface texture: Profile method. Rules and procedures for assessment of surface texture, 1998.

29. Gdańsk University of Technology, Faculty of Mechanical Engineering, www.pg.gda.pl/~kkrzysztof/struktura.html

30. Surface Roughness Tester SJ-301: User's Manual.

CONTACT WITH THE AUTHOR

Tomasz Hajduk

e-mail: t.hajduk@wm.am.gdynia.pl

Faculty of Marine Engineering
Gdynia Maritime University
Morska 81-87, 81-225
POLAND